[18F]flutemetamol amyloid positron emission tomography in preclinical and symptomatic Alzheimer's disease: Specific detection of advanced phases of amyloid-β pathology

Dietmar Rudolf Thal[a,*], Thomas G. Beach[b], Michelle Zanette[c], Kerstin Heurling[d,e], Aruna Chakrabarty[f], Azzam Ismail[f], Adrian P. L. Smith[g], Christopher Buckley[g]

[a]Institute of Pathology—Laboratory of Neuropathology, Center for biomedical Research, University of Ulm, Ulm, Germany
[b]Civin Laboratory for Neuropathology, Banner Sun Health Research Institute, Sun City, AZ, USA
[c]Life Sciences R&D Biometrics, GE Healthcare, Princeton, NJ, USA
[d]Life Sciences R&D, GE Healthcare, Uppsala, Sweden
[e]Department of Surgical Sciences: Radiology, Uppsala University, Uppsala, Sweden
[f]Pathology and Tumour Biology, Leeds Institute of Molecular Medicine, St. James Hospital, Leeds, UK
[g]Life Sciences R&D, GE Healthcare, Amersham, UK

Abstract

Background: Amyloid positron emission tomography (PET) has become an important tool to identify amyloid-β (Aβ) pathology in Alzheimer's disease (AD) patients. Here, we determined the diagnostic value of the amyloid PET tracer [18F]flutemetamol in relation to Aβ pathology at autopsy.

Methods: [18F]flutemetamol PET was carried out in a cohort of 68 patients included in a [18F]flutemetamol amyloid PET imaging end-of-life study (GE067-007). At autopsy, AD pathology was determined and Aβ plaque pathology was classified into phases of its regional distribution (0–5).

Results: [18F]flutemetamol PET was universally positive in cases with advanced stage postmortem Aβ pathology (Aβ phases 4 and 5). Negative amyloid PET was universally observed in nondemented or non-AD dementia cases with initial Aβ phases 1 and 2, whereas 33.3% of the phase 3 cases were positive.

Conclusions: [18F]flutemetamol amyloid PET detects primarily advanced stages of Aβ pathology in preclinical and symptomatic AD cases.

© 2015 The Authors. Published by Elsevier Inc. on behalf of the Alzheimer's Association. This is an open access article under the CC BY-NC-ND license (http://creativecommons.org/licenses/by-nc-nd/4.0/).

Keywords: Amyloid; Alzheimer's disease; Preclinical stage; Amyloid PET; [18F]flutemetamol

1. Introduction

Amyloid-β protein (Aβ) deposition is one of the hallmarks of Alzheimer's disease (AD) [1,2]. The in vivo detection of amyloid pathology in the human brain has become feasible by the use of [11C]- and [18F]-labeled amyloid binding ligands and positron emission tomography (PET) [3–6]. In vitro-labeling experiments with the [11C]-labeled amyloid tracer Pittsburg compound B (PIB) disclose plaques on histopathologic slides [7]. Autopsies performed on AD subjects that received amyloid PET before death have shown that areas with a high plaque density showed ligand retention with amyloid PET [8–10].

Neuropathologically, the deposition of Aβ plaques starts in the neocortex and then expands hierarchically into further brain regions [11]. In the second phase, allocortical plaques

occur, whereas in phase 3, additional plaques are found in the basal ganglia and in the diencephalon, in phase 4 in the midbrain and the medulla oblongata, and in the fifth and final phase also in the cerebellum and the pons. These phases of Aβ deposition are associated with the parallel development of neurofibrillary tangle (NFT) pathology in the course of preclinical and symptomatic AD. Aβ phases 4 and 5 are almost always associated with symptomatic AD [11]. The current guidelines of the National Institute of Aging and the Alzheimer Association (NIA-AA) for the neuropathologic diagnosis of AD recommend the assessment of the Aβ phases in concert with the Braak stages for NFT pathology (Braak-NFT stage) and the Consortium to establish a Registry for AD (CERAD) score for the assessment of the frequency of neuritic plaques [12]. According to these guidelines, Aβ deposition in the brain indicates the presence of AD pathology regardless of cognitive deficits [12]. Because clinical AD by definition is restricted to demented individuals [13], the diagnosis of preclinical AD (pre-AD) has been introduced for nondemented cases with positive AD biomarkers [14]. Histopathologically, detectable AD pathology in nondemented cases may, therefore, be classified as pathologically defined pre-AD (p-pre-AD) cases [15,16].

Until now, it was not clear whether amyloid PET uptake mirrors the hierarchical pattern of Aβ plaque deposition, and if so, which phases of Aβ pathology might be detectable with amyloid PET imaging techniques, or how accurate amyloid PET might be for the differential diagnosis between autopsy proven AD, p-pre-AD, non-AD dementias, such as vascular dementia, Lewy body disease (LBD) or frontotemporal lobar degeneration (FTLD), and nondemented non-AD cases. [^{18}F]flutemetamol is structurally similar to PIB [17] and has recently been validated for the detection of amyloid plaques [10]. We compared [^{18}F]flutemetamol amyloid PET with the amyloid plaque phase, neuritic plaque density, and associated NFT pathology in 68 autopsy cases enrolled in the [^{18}F] flutemetamol amyloid PET imaging end-of-life study (GE067-007).

2. Material and methods

2.1. Subjects

The subject cohort of 68 cases was included in the efficacy analysis of the GE-067-007 Phase 3 end-of-life clinical trial and autopsied after death (Table 1). Dementia, defined according to the *Diagnostic and Statistical Manual of Mental Disorders, Fourth Edition* (*DSM-IV*) criteria, was noted as present or absent. This was a phase 3, multicenter PET study of [^{18}F]flutemetamol injection for detecting brain Aβ (ClinicalTrials.gov identifier NCT01165554). Local institutional review boards or ethics committees approved the study protocol before initiation. All subjects or their legal representatives gave prior written informed consent/assent. Consecutive eligible subjects were ≥55 years of age, terminally ill with a life expectancy <1 year, and with general health adequate to undergo study procedures. Patients died of natural causes and serious adverse events were not attributable to [^{18}F]flutemetamol injection [10]. Subjects were ineligible if they were pregnant/lactating, had known/suspected structural brain abnormalities, contraindication(s) for PET, known/suspected hypersensitivity/allergy to [^{18}F]flutemetamol injection (or any component), or had participated in any clinical study using an investigational product within 30 days of signing consent. The scan-death intervals ranged between 0 and 397 days (mean 104 days; median 78 days).

2.2. Neuropathology assessments

Brain material received at autopsy and previously used for diagnostic purposes supporting the GE067-007 phase 3 clinical trial was examined. All brains were formalin fixed. The brains were cut in coronal slices and screened macroscopically for the presence of infarcts, hemorrhages, tumors, and inflammatory lesions. For histopathologic analysis and for assessing the amounts of AD-related amyloid plaques, NFTs, and neuritic plaques, we examined paraffin-embedded tissue including parts of the frontal, parietal, temporal, occipital cortex, and entorhinal cortex, the hippocampal formation at the level of the lateral geniculate body, basal ganglia, thalamus, amygdala, midbrain, pons, medulla oblongata, and cerebellum. Paraffin sections of 5 μm thickness from all blocks were stained with hematoxylin & eosin (H&E) and anti-Aβ antibodies (1:100, formic acid and heat pretreatment; anti-Aβ; 4G8, SIG-39220; Covance, USA). For neuropathologic diagnosis, sections were stained with the Bielschowsky silver method and immunohistochemical methods for abnormal phosphorylated tau protein (anti-human PHF-tau monoclonal antibody; AT8, prod. no. MN1020, 1:40; Thermo Scientific, UK), α-synuclein (anti-α-synuclein monoclonal antibody; prod. no. NCL-L-ASYN, lot no. 6005209, 1:40; Leica Microsystems, UK), and ubiquitin (anti-ubiquitin polyclonal antibody; prod no. Z0458, 1:400; DakoCytomation, UK). Primary antibodies were detected with biotinylated secondary antibodies (E0354, DakoCytomation) and visualized with the DABMap Kit (Ventana, USA). The phase of Aβ plaque pathology (Aβ phase) was assessed after screening the Aβ-stained sections for plaque distribution according to previously published protocols [11,18]. The neuropathologic diagnosis of AD pathology was performed as recommended (Table 2) [12]. Aβ plaques loads were determined in 32 cases as shown in Supplmentary Fig. 3.

Additional vascular changes were assessed in H&E-stained sections. LBD and multiple system atrophy–related changes were determined using α-synuclein immunohistochemistry. Other tauopathies (FTLD-tau) were diagnosed on the basis of antiabnormal tau protein–stained sections. Ubiquitin-stained sections were used to identify other types of FTLD or motor neuron disease.

Table 1
List of cases

Case number	Age, y	Sex	Neuropathologic diagnosis	Dementia	Clinicopathologic AD classification	Amyloid PET classification	Aβ phase	Braak stage	CERAD sore for neuritic plaques	NIA-AA degree of AD	Scan-death interval	$SUVR_{CER}$	$SUVR_{PONS}$
1	80	M	AD	+	AD	Positive	5	6	3	3	0	1.996	0.665
2	72	M	AD	+	AD	Positive	5	6	3	3	1	2.37	0.786
3	85	M	AD	+	AD	Positive	5	5	2	3	394	2.825	0.881
4	83	M	AD	+	AD	Positive	5	6	3	3	33	2.595	0.8
5	85	F	AD	+	AD	Positive	5	6	3	3	127	2.902	0.89
6	80	M	AD	+	AD	Positive	5	6	3	3	170	2.335	0.757
7*	88	F	AD, DLB	+	AD + non-AD dementia	Positive	5	6	2	3	78	1.674	0.663
8	76	F	AD, CAA	+	AD	Positive	5	6	3	3	26	1.832	0.683
9	65	F	AD	+	AD	Positive	5	6	3	3	139	2.366	0.822
10	74	M	AD, CAA	+	AD	Positive	5	4	2	2	372	1.476	0.54
11	78	M	AD, DLB	+	AD + non-AD dementia	Positive	5	6	2	3	61	2.859	0.872
12	80	M	AD, DLB	+	AD + non-AD dementia	Positive	5	6	1	2	2	2.101	0.793
13	78	F	AD, DLB	+	AD + Non-AD Dementia	Positive	5	6	3	3	124	2.122	0.697
14	73	F	AD	+	AD	Positive	5	6	3	3	26	2.228	0.7
15	84	M	AD, CAA, multiple infarcts	+	AD + non-AD dementia	Positive	5	6	2	3	59	2.81	0.958
16	94	F	AD	+	AD	Positive	5	3	1	2	19	1.953	0.741
17	87	M	AD	+	AD	Positive	5	6	3	3	105	2.201	0.728
18	95	F	AD	+	AD	Positive	5	6	2	3	14	1.887	0.863
19	83	F	AD	+	AD	Positive	5	5	2	3	193	2.399	0.79
20	87	F	DLB, AD	+	AD + non-AD dementia	Positive	5	4	1	2	130	1.95	0.736
21	86	F	AD	+	AD	Positive	5	5	3	3	154	2.426	0.946
22	75	F	AD	+	AD	Positive	5	6	3	3	65	2.465	0.886
23	88	F	AD, DLB, CAA, arteriolosclerosis	+	AD + non-AD dementia	Positive	5	6	2	3	114	2.385	0.874
24	81	F	AD, DLB	+	AD + non-AD dementia	Positive	4	4	2	2	126	2.323	0.99
25	80	M	AD	+	AD	Positive	4	6	2	3	276	2.334	0.861
26	87	M	AD	+	AD	Positive	4	4	2	2	22	2.041	0.623
27	89	M	AD pathology, DLB	+	Non-AD dementia	Positive	4	2	2	1	307	2.186	0.708
28	82	M	AD, CAA	+	AD	Positive	4	6	3	3	14	2.234	0.741
29	77	F	AD pathology, LBD	+	Non-AD dementia	Positive	4	1	3	1	179	2.03	0.688
30	87	F	AD pathology, DLB, arteriolosclerosis, infarct	+	Non-AD dementia	Positive	4	2	1	1	118	3.137	0.862
31	83	F	AD	+	AD	Positive	4	6	3	3	198	1.483	0.594
32	90	F	AD	+	AD	Positive	4	6	3	3	50	2.349	0.868
33	77	F	AD	+	AD	Positive	4	6	3	3	10	1.59	0.879
34	91	F	AD, CAA	+	AD	Positive	4	6	3	3	55	2.2	0.748
35	91	M	AD	+	AD	Positive	4	5	2	3	29	1.857	0.614
36	81	M	AD, DLB, CAA	+	AD + non-AD dementia	Positive	4	6	3	3	204	2.414	0.815
37	91	F	AD, DLB	+	AD + non-AD dementia	Positive	4	3	1	2	131	2.719	0.785
38	87	M	AD, CAA	+	AD	Positive	4	4	3	2	1	2.098	0.822

(*Continued*)

Table 1
List of cases (*Continued*)

Case number	Age, y	Sex	Neuropathologic diagnosis	Dementia	Clinicopathologic AD classification	Amyloid PET classification	Aβ phase	Braak stage	CERAD sore for neuritic plaques	NIA-AA degree of AD	Scan-death interval	SUVR$_{CER}$	SUVR$_{PONS}$
39	**85**	**F**	**AD, DLB**	**+**	**AD + non-AD dementia**	**Positive**	**4**	**3**	**2**	**2**	**192**	**2.067**	**0.655**
40	**79**	**M**	**AD pathology, CAA, metastatic carcinoma**	**−**	**p-pre-AD**	**Positive**	**4**	**3**	**2**	**2**	**41**	**2.441**	**0.898**
41*	91	F	AD pathology, CAA, LBD	+	Non-AD dementia	Negative	4	2	1	1	209	1.549	0.598
42	60	M	AD pathology, CAA (focal)	+	Non-AD dementia	Negative	4	2	1	1	10	1.083	0.372
43	**76**	**M**	**DLB**	**+**	**Non-AD dementia**	**Positive**	**3**	**2**	**2**	**1**	**83**	**1.874**	**0.737**
44	**81**	**F**	**DLB, AD**	**+**	**AD + non-AD dementia**	**Positive**	**3**	**4**	**2**	**2**	**183**	**1.661**	**0.646**
45	**84**	**M**	**Vascular dementia**	**+**	**Non-AD dementia**	**Positive**	**3**	**2**	**2**	**1**	**44**	**1.851**	**0.591**
46	92	M	DLB	−	p-pre-AD	Negative	3	2	2	1	322	1.355	0.482
47	72	F	DLB	−	p-pre-AD	Negative	3	1	2	1	294	1.76	0.589
48	71	M	PiD	+	Non-AD dementia	Negative	3	0	1	1	142	1.014	0.339
49	86	M	AD	+	AD	Negative	3	3	2	2	18	1.451	0.503
50	87	F	Vascular dementia	+	Non-AD dementia	Negative	3	1	1	1	76	1.569	0.493
51	75	M	DLB, infarcts	+	Non-AD dementia	Negative	3	2	2	1	63	1.227	0.44
52	74	M	Multiple infarct dementia	+	Non-AD dementia	Negative	2	0	0	1	169	1.119	0.365
53	84	F	Vascular dementia	+	Non-AD dementia	Negative	2	2	1	1	68	1.363	0.502
54	86	F	Aging changes, arteriolosclerosis	+	Non-AD dementia	Negative	2	0	1	1	136	1.527	0.47
55	89	F	CAA, NFT-predominant dementia, AD pathology	+	Non-AD dementia	Negative	2	4	1	1	77	1.252	0.408
56	75	F	Normal	+	Non-AD dementia	Negative	2	1	0	1	9	1.558	0.536
57	89	F	Infarct, arteriolosclerosis	+	Non-AD dementia	Negative	1	3	1	1	114	1.404	0.379
58*	72	F	NFT-predominant dementia	+	Non-AD dementia	Negative	1	5	0	1	104	1.343	0.409
59*	82	F	DLB	+	Non-AD dementia	Negative	1	3	1	1	24	1.723	0.458
60	76	F	DLB, vascular dementia	+	Non-AD dementia	Negative	1	2	0	1	145	1.218	0.408
61	60	F	Normal	−	p-pre-AD	Negative	1	0	0	1	34	1.669	0.589
62	84	M	Normal	+	Non-AD dementia	Negative	0	1	0	0	16	1.18	0.371
63	91	M	Vascular dementia, early stage PSP	+	Non-AD dementia	Negative	0	0	0	0	130	1.344	0.4
64	66	M	Aging changes	+	Non-AD dementia	Negative	0	0	0	0	154	1.298	0.453
65	70	M	Normal	−	Non-AD	Negative	0	0	0	0	15	1.44	0.489
66	63	M	Normal	−	Non-AD	Negative	0	0	0	0	12	1.597	0.473
67	67	M	Normal	−	Non-AD	Negative	0	1	0	0	32	1.369	0.466
68*	79	M	AGD	+	Non-AD dementia	Negative	0	3	0	0	130	1.259	0.445

Abbreviations: M, male; F, female; AD, Alzheimer's disease; PET, positron emission tomography; Aβ, amyloid-β; NIA-AA, National Institute of Aging and the Alzheimer Association; SUVR$_{CER}$, cerebellum standard uptake value ratio; SUVR$_{PONS}$, pons cerebellum standard uptake value ratio; DLB, Dementia with Lewy Bodies; CAA, cerebral amyloid angiopathy; LBD, Lewy Body Disease (includes DLB); PiD, Pick's Disease (FTLD-tau subtype); NFT, neurofibrillary tangle; PSP, pregressive supranuclear palsy (FTLD-tau subtype); AGD, Argyrophilic Grain Disease (FTLD-tau subtype).

NOTE. Cases with a positive [^{18}F]flutemetamol amyloid PET were given in boldface. Case numbers marked with "*" indicate cases who received 185 MBq. All other cases received an injection of 370 MBq [^{18}F]flutemetamol. Dementia: "+" indicates demented; "−" indicates not demented. Aβ-phase, Braak-NFT Stage, CERAD Neuritic Plaque Score, and NIA-AA degree of AD Pathology were determined as previously published [11,12,35,36]. Scan-death interval in days.

Table 2
Pathologic and clinicopathologic classification criteria as applied in this study

A: Amyloid score (amyloid plaque phase)	C: CERAD (neuritic plaque score)	B: NFT score (Braak-NFT stage)		
		B0 or B1 (I/II)	B2 (III/IV)	B3 (V/VI)
A0 (0)	C0 (0)	No AD	No AD	No AD
A1 (1/2)	C0/1 (0/1)	Low	Low	Low
	C2/3 (2/3)	Low	Intermediate	Intermediate
A2 (3)	Any C	Low	Intermediate	Intermediate
A3 (4/5)	C0/1 (0/1)	Low	Intermediate	Intermediate
	C2/3 (2/3)	Low	Intermediate	High

	No AD/no PART	PART	NFT-predominant dementia	p-pre-AD	Symptomatic AD	Symptomatic AD + non-AD dementia	Non-AD dementia
B score	0	B1–B2	B2–B3	B0–B3	B2–B3	B2–B3	B0–B2
Degree of AD pathology	No AD	No AD	No AD or low	Low–high	Intermediate–high	Intermediate–high	No AD or low
Clinical signs of dementia or cognitive decline	No	No	Yes	No	Yes	Yes	Yes
Dementing disorder other than AD	No	No	Yes (NFT-predominant dementia)	No	No	Yes	Yes

Abbreviations: NFT, neurofibrillary tangle; AD, Alzheimer's disease; PART, primary age-related tauopathy; p-pre-AD, pathologically defined pre-AD.

NOTE. A: Determination matrix for the NIA-AA Degree of AD pathology regardless of the clinical status as previously published [12]. Aβ phase, Braak-NFT stage and CERAD score for neuritic plaques are required to determine the NIA-AA degree of AD pathology [11,35,36].

B: Subclassification of p-preAD, symptomatic AD, symptomatic AD with non-AD dementia (i.e. mixed dementia), non-AD dementia, definite PART and definite NTF-predominant dementia with respect of the clinical status [13,14,16,19,37,38].

There may be overlap between p-pre-AD and PART if one does not restrict to definite PART without any Ab pathology as done here. NFT-predominant dementia has been included in PART but an alternative classification for FTLD terms demented cases with this type of pathology NFT-predominant dementia [19,37]. To avoid confusion, we used the term NFT-predominant dementia for the demented "PART" cases.

2.3. Clinicopathologic classification of cases

Demented cases with at least intermediate NIA-AA degrees of AD pathology [12] were considered as symptomatic AD cases; nondemented individuals with AD pathology were referred to as p-pre-AD cases as previously suggested [15,16] (Table 2). Nondemented cases without AD pathology were classified as non-AD controls. Non-AD controls included cases with NFT pathology in the medial temporal lobe that recently has been termed primary age-related tauopathy [19] (Table 2). Patients with non-AD dementia encompassed demented patients with vascular dementia, LBD, and FTLD-tau (argyrophilic grain disease, NFT-predominant dementia, Pick's disease) that did not exhibit intermediate or high degrees of AD pathology indicating that AD pathology was presumably not responsible for dementia. Cases with intermediate or high degrees of AD pathology and apparent lesions of a second dementia-related disorder were classified as a subgroup of AD cases: AD + non-AD dementia (identical with mixed dementia; Table 2).

2.4. [^{18}F]flutemetamol PET image assessments

Amyloid PET imaging was performed at 12 different imaging sites (Supplementary Methods). Before PET imaging, subjects underwent head computed tomography (CT) or magnetic resonance imaging, unless prior images (obtained within 12 months) were available. [^{18}F]flutemetamol injection was administered intravenously at a dose of 185 or 370 MBq of radioactivity at physician discretion (Supplementary Methods). PET images were acquired in 2-minute frames on PET/CT cameras, beginning approximately 90 minutes after injection. Five frames were summed to give a 10-minute scan, which was attenuation corrected using CT data. Equipment used to capture images varied across the 12 imaging sites (Supplementary Methods). Most images were reconstructed iteratively to form 128 × 128 axial slices, and a Gaussian post-reconstruction smoothing filter was applied to some. The images were evaluated over all as either positive or negative for amyloid by five independent readers blinded to all clinical, demographic, and pathology information. The readers were experienced nuclear medicine physicians or radiologists scoring PET images with knowledge of the respective CT scans. The results reported here are using the majority read for global classification of the GE067-007 images from a reread study (GE-067-021) after automated reader training (Supplementary Fig. 1, Supplementary Methods).

The [^{18}F]flutemetamol standard uptake values (SUVs) were measured for five volumes of interest (VOIs) restricted to gray matter and adjusted for atrophy manually, covering the anterior cingulate, the prefrontal cortex, the lateral temporal cortex, the parietal cortex, and one VOI covering both posterior cingulate and precuneus (Supplementary Fig. 2). Frame-to-frame motion correction was performed on the dy-

namic data before quantitative SUV measurements and standard uptake value ratio (SUVR) calculations were made. As reference for cerebellum SUV (SUVR$_{CER}$), the cerebellar gray matter SUV was used. To exclude bias by using the cerebellar gray matter as reference, we also obtained SUV for the pons as a reference. SUVRs were calculated as a ratio of cortical region SUV to either the SUVR$_{CER}$ reference or pons SUV reference (SUVR$_{PONS}$). A global cortical average (composite SUVR) was calculated averaging the cortical SUVRs. Image processing and VOI analysis were performed using voyager 4 (GE Healthcare, Uppsala, Sweden).

2.5. Statistical analysis

Logistic regression analysis, analysis of variance (ANOVA) and Fisher's exact test were calculated using SPSS 21 statistical software (IBM, Armonk, NY, USA) (Supplementary Methods).

3. Results

3.1. [^{18}F]flutemetamol amyloid PET: Association with Aβ-phases

Most (89%) Aβ phase 4 and all Aβ phase 5 cases exhibited a positive amyloid PET signal, whereas all Aβ phase 0, 1, and 2 cases showed a negative PET. Only 33.3% of the Aβ phase 3 cases exhibited a positive amyloid PET (Fig. 1, Table 1). This finding was confirmed by measuring Aβ plaque loads in 32 of our cases providing a threshold of an Aβ plaque load of 5% for [^{18}F]flutemetamol amyloid PET
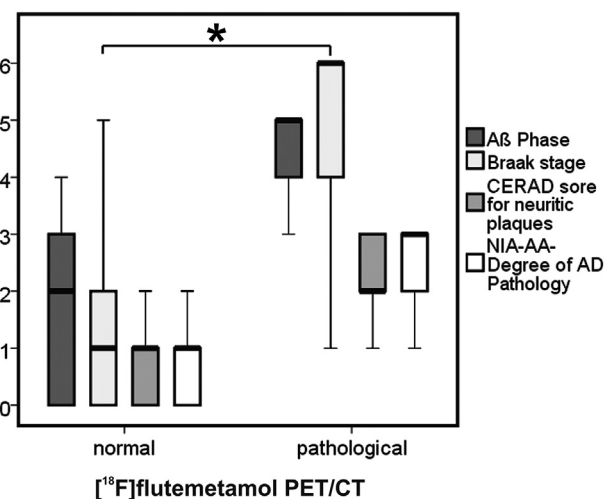

Fig. 1. Boxplot diagram of Aβ phase, Braak-NFT stage, CERAD score for neuritic plaque pathology and the NIA-AA degree of AD pathology for cases with negative (n = 25) and positive amyloid PET pattern (n = 43). *$P < .05$ in a logistic regression model controlled for age, sex, scan-death interval, and Braak-NFT stage. Abbreviations: NFT, neurofibrillary tangle; NIA-AA, National Institute of Aging and the Alzheimer Association; AD, Alzheimer's disease; PET, positron emission tomography; Aβ, amyloid-β; CT, computed tomography.

positivity (Supplementary Fig. 3). Likewise, high Braak-NFT stages and high CERAD neuritic plaques scores as well as high and intermediate NIA-AA degrees of AD pathology were observed in cases with positive PET uptake, whereas cases with a negative amyloid PET exhibited either no or only low degrees of NFT, neuritic plaque pathology as well as low NIA-AA degrees AD pathology or no AD pathology (Fig. 1, Table 1).

Two cases with NFT-predominant dementia with Braak-NFT stages IV and V showed a negative amyloid PET. Higher densities of neuritic plaques (moderate or frequent) were commonly found in AD cases with a positive amyloid PET although 13 cases with a sparse to moderate neuritic plaque density had negative amyloid PET scans (Table 1).

In a logistic regression model controlled for age, sex, and scan-death interval Aβ phases had a significant influence on the amyloid PET pattern, whereas NFT stages did not show a significant effect on the amyloid PET pattern (Aβ phases: $P = .006$, odds ratio [OR]: 12.98, 95% confidence interval [CI]: 2.065–81.583; Braak-NFT stages: $P = .092$). The CERAD score for neuritic plaque density was not integrated in this model because of collinearity with the Aβ plaque phase. A significant association between the amyloid PET pattern, on the one hand, the Braak-NFT stage and the CERAD neuritic plaque density score, on the other, was observed in separate models without Aβ-phase (Braak-NFT stages: $P < .001$, OR: 3.275, 95% CI: 1.886–5.687; CERAD score: $P < .001$, OR: 21.023, 95% CI: 4.026–109.772). These results were expected from previously published data examining the associations between NFT pathology and neuritic and Aβ plaque pathology [15,20].

In agreement with the dichotomous [18F]flutemetamol PET assessment as negative or positive, cortical composite $SUVR_{CER}$ did not show differences among individual Aβ phase 0–2 subjects (Fig. 2; $SUVR_{CER} < 1.6$ except two phase 1 cases: 1.67, 1.72). Phase 3 subjects rated as positive had $SUVR_{CER}$ levels between 1.66 and 1.87. Cases with negative PET assessment had $SUVR_{CER}$ levels <1.6 except for one case with a $SUVR_{CER}$ of 1.76 (Fig. 2). Cases with Aβ phases 4 and 5 identified as having a positive amyloid [18F]flutemetamol retention pattern had increased cortical $SUVR_{CER}$ (>1.6). Only two phase 4 (1.48 and 1.59) and one phase 5 case had lower $SUVR_{CER}$ levels (1.48). The two Aβ phase 4 cases with a negative [18F]flutemetamol PET exhibited $SUVR_{CER}$ levels <1.6. Overall, cases with Aβ phases 4 and 5 had significantly higher SUVRs than those in lower phases (ANOVA $P \leq .006$, corrected for multiple testing with Games-Howell post hoc test). Similar differences have been found when using $SUVR_{PONS}$ instead of $SUVR_{CER}$ for statistical analysis (Supplementary Table 1).

3.2. [18F]flutemetamol amyloid PET differentiates AD cases from non-AD dementia, p-pre-AD, and no AD cases

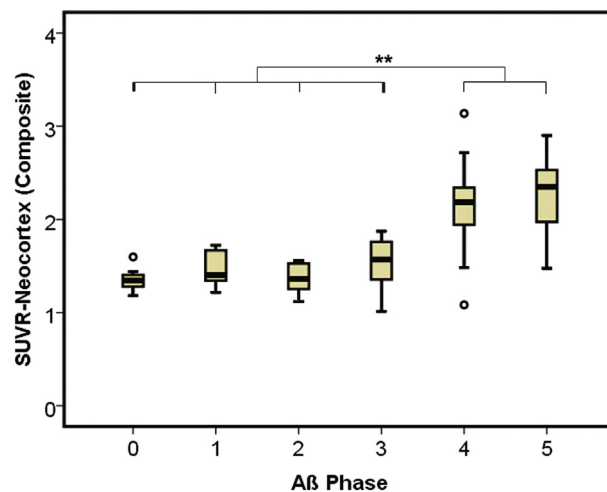Positive amyloid PET scans were obtained in all cases with AD-type mixed dementia, i.e. cases with intermediate

Fig. 2. Composite neocortical $SUVR_{CER}$ levels of [18F]flutemetamol retention do not increase significantly until and including Aβ phase 3 but are significantly increased in cases of Aβ phases 4 and 5. Circles represent outliers. **$P < .01$. (Aβ phase 0: n = 7; Aβ phase 1: n = 5; Aβ phase 2: n = 5; Aβ phase 3: n = 9; Aβ phase 4: n = 19; and Aβ phase 5: n = 23). Abbreviations: $SUVR_{CER}$, cerebellum standard uptake volume ratio; Aβ, amyloid-β.

to high AD pathology according to the NIA-AA criteria and significant signs of a second dementing disorder (Fig. 3A, Tables 1 and 2) and in 96.2% of the pure AD cases. Only one demented case with intermediate AD pathology did not exhibit a positive PET signal. This case exhibited Aβ phase 3 (Table 1).

One of four nondemented p-pre-AD cases (25%) exhibited a positive amyloid PET (Fig. 3A, Table 1). In non-AD dementia cases with no or low degrees of AD pathology amyloid PET images were positive in 21.7% (Fig. 3A, Table 1) and such cases exhibited Aβ phase 3 or 4 (Fig. 3A, Table 1).

Binary logistic regression analysis in a model controlled for age, sex, and scan-death interval revealed that positive [18F]flutemetamol amyloid PET uptake patterns identified symptomatic AD cases including those with additional non-AD pathology rather than nondemented p-pre-AD and non-AD controls ($P = .008$; OR: 143.05; 95% CI: 4.681–4371.714). Likewise, symptomatic AD (including those cases with additional non-AD pathology) was distinguished from pure non-AD dementias ($P < .002$; OR: 155.199; 95% CI: 15.541–1549.928). Differences in the $SUVR_{CER}$ levels confirmed the distinction of AD cases (including cases with fully developed AD pathology and additional non-AD pathology) from non-AD, and non-AD dementia cases (Fig. 3B; ANOVA $P \leq .001$, corrected for multiple testing with Games-Howell post hoc test). Subjects with p-pre-AD (n = 4) were not distinguished from nondemented control subjects (n = 3) by [18F]flutemetamol amyloid PET pattern ($P = 1.0$, Fisher's exact test) or by $SUVR_{CER}$ differences (Fig. 3; $P = .655$, ANOVA corrected for multiple testing with Games-Howell post hoc test) in our sample. Similar results have been obtained
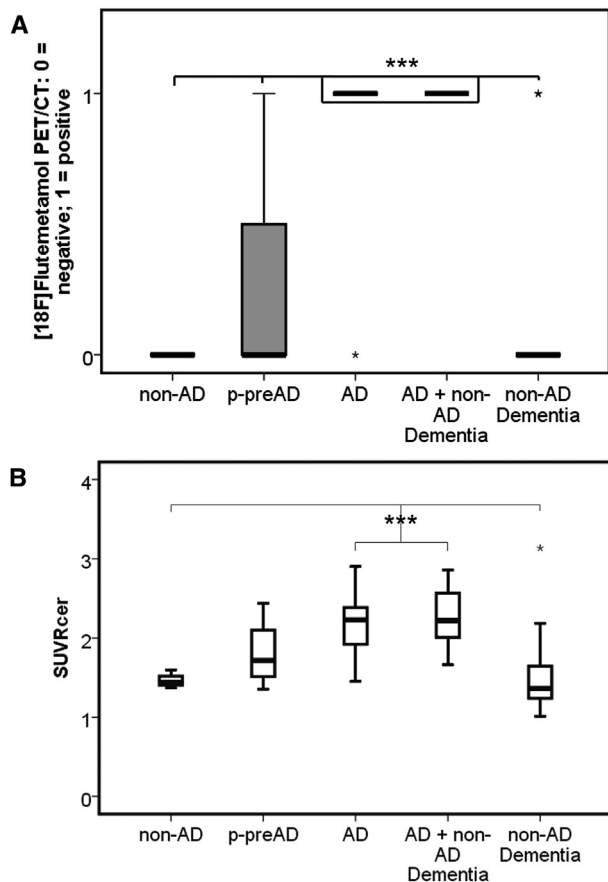
Fig. 3. (A) Boxplot diagram showing the distributions of negative and positive [¹⁸F]flutemetamol amyloid PET pattern in non-AD, p-pre-AD, symptomatic AD with and without copathology of other dementing disorders, and in non-AD dementia cases (i.e., FTLD, vascular dementia, and LBD). AD cases with and without copathology exhibited positive [¹⁸F]flutemetamol amyloid PET pattern, whereas non-AD, p-pre-AD, and non-AD dementia cases did not. (B) Composite [¹⁸F]flutemetamol SUVR$_{CER}$ levels confirmed the increase in [¹⁸F]flutemetamol retention in AD cases with or without additional dementia-related pathologies in comparison to non-AD and non-AD dementia cases. *= outlier. ***$P <.0001$. (non-AD controls: n = 3; p-pre-AD: n = 4; AD: n = 26; AD + non-AD dementia: n = 12; and non-AD dementia: n = 23). Abbreviations: PET, positron emission tomography; AD, Alzheimer's disease; p-pre-AD, pathologically defined pre-AD; FTLD, frontotemporal lobar degeneration; LBD, Lewy body disease; SUVR$_{CER}$, cerebellum standard uptake volume ratio; CT, computed tomography.

when using SUVR$_{PONS}$ instead of SUVR$_{CER}$ for statistical analysis (Supplementary Table 1).

4. Discussion

The key novel finding in this study is that [¹⁸F]flutemetamol amyloid PET detects Aβ pathology only in cases with advanced phases of plaque pathology at autopsy, that is, primarily Aβ phases 4 and 5 (Fig. 4). This finding was confirmed by measuring Aβ plaque loads as shown in Supplementary Fig. 3. An additional major finding is that [¹⁸F]flutemetamol amyloid PET primarily detects Aβ plaque pathology in AD cases with advanced stage Aβ pathology

representing Aβ phases 4 and 5 permitting the distinction between AD and non-AD dementias. In contrast, p-pre-AD cases with Aβ phases 1–2 did not exhibit a positive [¹⁸F]flutemetamol PET pattern and did not differ in cortex SUVR$_{CER}$ levels from non-AD control cases (Fig. 3 and 4). Only three of nine Aβ phase 3 cases exhibited a positive imaging pattern, and each of these cases was demented. Only one nondemented case with a positive [¹⁸F]flutemetamol amyloid PET was observed. However, this case had significant AD pathology with Aβ phase 4 and Braak-NFT stage III. As such, given the current rating protocols [¹⁸F]flutemetamol amyloid PET analysis allowed a clear cut distinction of >95% of the symptomatic AD subjects with or without additional neurodegenerative pathology from cases free of AD pathology, p-pre-AD cases and cases with non-AD dementias, that is, FTLD, LBD, and vascular dementia. Amyloid PET did not allow a distinction between pure AD cases and AD cases with additional LBD or additional vascular pathology, most likely because both groups exhibited Aβ phases 4 or 5. It is well known that amyloid tracers detect plaque pathology in a subgroup of aged nondemented individuals [21–24]. Our finding that only those nondemented cases with Aβ pathology representing advanced phases (i.e., phase 3 and higher) were identified by [¹⁸F]flutemetamol amyloid PET points to the interpretation that amyloid PET detects only a subgroup of the p-pre-AD cases: those cases that are close to the threshold of symptomatic AD. Aβ plaque load measurements confirmed this interpretation. This finding is in line with the report of amyloid PET-negative cases already showing AD-related cerebrospinal fluid Aβ changes [25].

Furthermore, amyloid PET with florbetapir (another amyloid tracer) was reported to be positive in cases considered neuropathologically as definite or probable AD, whereas cases categorized as no AD or possible AD with Aβ plaque loads up to 1.14% did not exhibit a positive florbetapir PET [9]. Because densitometric measurements of immunoreactivity in general depend on the staining and cutting protocols as well as on correction filters and threshold settings [26] and vary among different laboratories [27], Aβ plaque loads determined here and by Clark et al. [9] cannot be compared directly with one another. Thus, threshold differences of approximately 3%–4% between both studies do not necessarily contradict the comparability of both tracers with PIB as previously published [28]. In this study we, therefore, chose the phases of Aβ plaque distribution [11] as a parameter for Aβ plaque pathology. This has proven to generate highly reliable and valid information on the amount of Aβ plaque pathology as demonstrated in interlaboratory and interrater studies by BrainNet Europe [18,29]. The increased likelihood of future cognitive decline in amyloid PET-positive nondemented individuals [21–24] is in agreement with the detection of advanced stage Aβ pathology in the nondemented individuals as seen in our autopsy study.
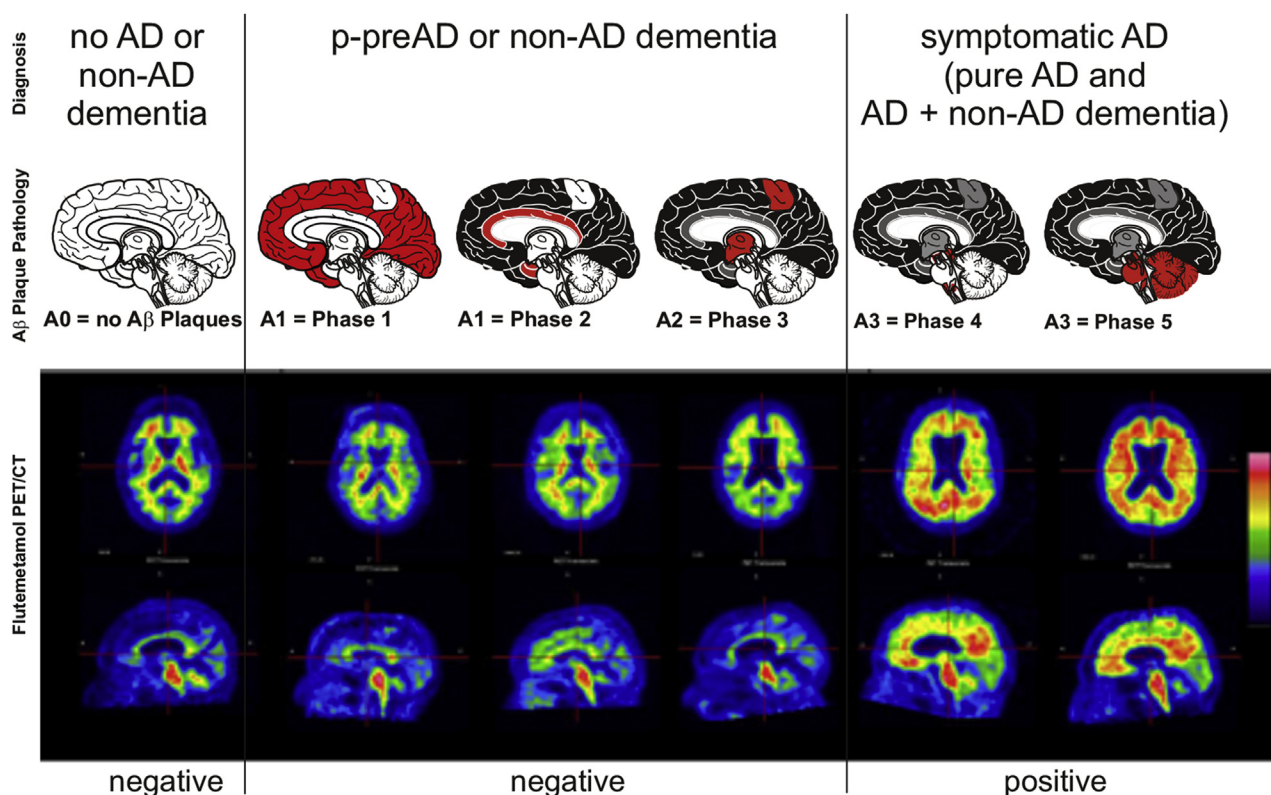
Fig. 4. Schematic representation of Aβ plaque pathology in different Aβ phases with corresponding [^{18}F]flutemetamol amyloid PET images. Cases with early Aβ phases 1–3 did not exhibit a significant [^{18}F]flutemetamol retention, whereas symptomatic or preclinical AD cases with Aβ phases 4 and 5 showed positive [^{18}F]flutemetamol retention. Parts of this figure are reproduced with permission from Thal DR, et al. Phases of Abeta-deposition in the human brain and its relevance for the development of AD. Neurology 2002;58:1791–800. [11]. Abbreviations: Aβ, amyloid-β; PET, positron emission tomography; AD, Alzheimer's disease; p-pre-AD, pathologically defined pre-AD.

In vivo [^{18}F]flutemetamol binding was reported for amyloid plaques in Tg2576 mice and in AD patients [30–32]. The fact that cortical Aβ plaques and neuritic plaques in Aβ phase 1 and 2 cases as well as in 66.7% of the Aβ phase 3 cases were not detected by [^{18}F]flutemetamol PET demonstrates that amyloid PET is not sensitive enough to detect initial stages of these pathologies. Only increased numbers of cortical plaques usually associated with increased amounts of cortical soluble and nonplaque-associated insoluble (so called dispersible) Aβ aggregates in Aβ phase 4 and 5 cases [15,16] permitted significant [^{18}F]flutemetamol retention in the cortex. The assumption of a threshold for Aβ pathology to be passed for detection with amyloid PET is in agreement with the negative PIB amyloid imaging results in aged monkeys with amyloid plaques that may not exhibit sufficient degrees of amyloid pathology (as Aβ phase 1–3 cases in this study) to allow detection by amyloid PET methods [33].

Based on composite SUVR$_{CER}$ of cortical regions [^{18}F] flutemetamol amyloid PET was not sensitive enough for the detection of the hierarchical pattern of Aβ plaque expansion in the human brain seen neuropathologically [11]. This finding is in line with that of other authors [34] and highlights the fact that amyloid PET is not as precise as the gold standard of neuropathologic analysis and should be interpreted carefully as only bulk effects will be identified, whereas minor effects may be difficult to detect. Moreover, our finding of no significant increase of cortical composite SUVR$_{CER}$ between Aβ phases 0–3 points to interindividual SUVR differences that should not be misinterpreted as early Aβ deposition in studies without pathologic confirmation. More detailed studies of pathology and amyloid PET in nondiseased individuals will be required to identify algorithms to distinguish no AD from p-pre-AD cases.

The use of the cerebellum or the pons as reference regions for SUVR calculation and the inclusion of only cortical regions into composite SUVRs preclude the detection of amyloid deposits in these regions characteristic for end-stage AD [11] and explain the failure of current amyloid PET rating strategies in the detections of a hierarchical pattern of Aβ deposition. For this purpose, SUVR levels of the brain stem, basal ganglia, and the thalamus would be required as well.

The selection of cerebellum or pons as reference regions, however, appears to be reasonable for amyloid PET given the fact that these two regions are the last to develop Aβ plaques in end-stage AD, whereas all other brain regions are affected earlier. Composite SUVR$_{CER}$ and SUVR$_{PONS}$,

thereby, showed similar effects related to the Aβ phases (Supplementary Table 1).

The neuritic plaque density as determined by the CERAD semiquantitative score confirmed the association of the amyloid PET pattern with the plaque load as described in detail by Curtis et al. [10]. All amyloid PET-positive cases had at least sparse neuritic plaques. [18F]flutemetamol PET did not detect severe abnormal tau pathology in cases with NFT-predominant dementia in line with previously published data for PIB [8].

One limitation in this study is the variable delay between the last PET scan and death, ranging between 0 and 397 days (mean 104 days; median 78 days), during which AD pathology could have progressed. To minimize the potential error induced by variable scan-death intervals, we included this parameter in the logistic regression model, although our cohort had shorter average scan-death interval compared to a similar study which had a scan-death interval up to 2 years [9].

Our finding that a distinct subgroup of p-pre-AD cases with very early phases of Aβ deposition was not detected by [18F]flutemetamol amyloid PET indicates that p-pre-AD cases can be subdivided into amyloid PET-positive clinically detectable cases and amyloid PET-negative presumably clinically "normal" p-pre-AD cases. The fact that [18F]flutemetamol PET tracer retention was restricted to cases with already advanced stages of Aβ pathology (Aβ phase 3 and higher) may have an impact on the interpretation and design of clinical studies in amyloid PET-positive nondemented individuals because at this stage the amyloid load is already high.

In summary, by identifying amyloid phase 4 and 5 cases, [18F]flutemetamol PET is well suited to detect amyloid pathology in symptomatic AD and mixed dementia cases with a significant AD component. Nondemented cases with a positive amyloid PET included in this study had advanced Aβ pathology at autopsy and, therefore, represent pathologically and clinically diagnosed pre-AD cases. Amyloid PET-negative p-pre-AD cases were related to the very early phases of Aβ pathology. However, such amyloid PET-negative p-pre-AD cases do already show initial AD pathology at autopsy.

Acknowledgments

Supplementary data

Supplementary data related to this article can be found at http://dx.doi.org/10.1016/j.jalz.2015.05.018.

RESEARCH IN CONTEXT

1. Systemic review: The authors reviewed literature related to amyloid positron emission tomography (PET) in Alzheimer's disease (AD) and its relation to neuropathologic lesions using PubMed and Google Scholar. Relevant work has been cited.

2. Interpretation: Our findings indicate that amyloid PET is an excellent tool for the differential diagnosis between AD and non-AD dementia cases. Moreover, we provide evidence that amyloid PET currently identifies pathologically diagnosed preclinical AD (p-pre-AD) cases at an already advanced point in the evolution of the disease.

3. Future directions: The use of amyloid PET to identify patients with preclinical phases of AD for therapeutic trials selects already biologically advanced phases of p-pre-AD. It is, therefore, essential to generate algorithms for amyloid PET assessment that enable detection of early phases of Aβ pathology.

References

[1] Glenner GG, Wong CW. Alzheimer's disease: Initial report of the purification and characterization of a novel cerebrovascular amyloid protein. Biochem Biophys Res Commun 1984;120:885–90.

[2] Masters CL, Simms G, Weinman NA, Multhaup G, McDonald BL, Beyreuther K. Amyloid plaque core protein in Alzheimer disease and Down syndrome. Proc Natl Acad Sci U S A 1985;82:4245–9.

[3] Klunk WE, Engler H, Nordberg A, Wang Y, Blomqvist G, Holt DP, et al. Imaging brain amyloid in Alzheimer's disease with Pittsburgh Compound-B. Ann Neurol 2004;55:306–19.

[4] Rinne JO, Wong DF, Wolk DA, Leinonen V, Arnold SE, Buckley C, et al. [(18)F]Flutemetamol PET imaging and cortical biopsy histopathology for fibrillar amyloid beta detection in living subjects with normal pressure hydrocephalus: Pooled analysis of four studies. Acta Neuropathol 2012;124:833–45.

[5] Zeng F, Goodman MM. Fluorine-18 radiolabeled heterocycles as PET tracers for imaging beta-amyloid plaques in Alzheimer's disease. Curr Top Med Chem 2013;13:909–19.

[6] Choi SR, Schneider JA, Bennett DA, Beach TG, Bedell BJ, Zehntner SP, et al. Correlation of amyloid PET ligand florbetapir F 18 binding with Abeta aggregation and neuritic plaque deposition in postmortem brain tissue. Alzheimer Dis Assoc Disord 2012;26:8–16.

[7] Klunk WE, Lopresti BJ, Ikonomovic MD, Lefterov IM, Koldamova RP, Abrahamson EE, et al. Binding of the positron emission tomography tracer Pittsburgh compound-B reflects the amount of amyloid-beta in Alzheimer's disease brain but not in transgenic mouse brain. J Neurosci 2005;25:10598–606.

[8] Ikonomovic MD, Klunk WE, Abrahamson EE, Mathis CA, Price JC, Tsopelas ND, et al. Post-mortem correlates of in vivo PiB-PET amyloid imaging in a typical case of Alzheimer's disease. Brain 2008; 131:1630–45.

[9] Clark CM, Pontecorvo MJ, Beach TG, Bedell BJ, Coleman RE, Doraiswamy PM, et al. Cerebral PET with florbetapir compared with

neuropathology at autopsy for detection of neuritic amyloid-beta plaques: a prospective cohort study. Lancet Neurol 2012;11:669–78.

[10] Curtis C, Gamez JE, Singh U, Sadowsky CH, Villena T, Sabbagh MN, et al. Phase 3 trial of flutemetamol labeled with radioactive fluorine 18 imaging and neuritic plaque density. JAMA Neurol 2015;72:287–94.

[11] Thal DR, Rüb U, Orantes M, Braak H. Phases of Abeta-deposition in the human brain and its relevance for the development of AD. Neurology 2002;58:1791–800.

[12] Hyman BT, Phelps CH, Beach TG, Bigio EH, Cairns NJ, Carrillo MC, et al. National Institute on Aging–Alzheimer's Association guidelines for the neuropathologic assessment of Alzheimer's disease. Alzheimers Dement 2012;8:1–13.

[13] McKhann GM, Knopman DS, Chertkow H, Hyman BT, Jack CR Jr, Kawas CH, et al. The diagnosis of dementia due to Alzheimer's disease: Recommendations from the National Institute on Aging-Alzheimer's Association workgroups on diagnostic guidelines for Alzheimer's disease. Alzheimers Dement 2011;7:263–9.

[14] Sperling RA, Aisen PS, Beckett LA, Bennett DA, Craft S, Fagan AM, et al. Toward defining the preclinical stages of Alzheimer's disease: Recommendations from the National Institute on Aging-Alzheimer's Association workgroups on diagnostic guidelines for Alzheimer's disease. Alzheimers Dement 2011;7:280–92.

[15] Thal DR, von Arnim C, Griffin WS, Yamaguchi H, Mrak RE, Attems J, et al. Pathology of clinical and preclinical Alzheimer's disease. Eur Arch Psychiatry Clin Neurosci 2013;263(Suppl 2):S137–45.

[16] Rijal Upadhaya A, Kosterin I, Kumar S, Von Arnim C, Yamaguchi H, Fändrich M, et al. Biochemical stages of amyloid β-peptide aggregation and accumulation in the human brain and their association with symptomatic and pathologically-preclinical Alzheimer's disease. Brain 2014;137:887–903.

[17] Vandenberghe R, Van Laere K, Ivanoiu A, Salmon E, Bastin C, Triau E, et al. 18F-flutemetamol amyloid imaging in Alzheimer disease and mild cognitive impairment: A phase 2 trial. Ann Neurol 2010;68:319–29.

[18] Alafuzoff I, Thal DR, Arzberger T, Bogdanovic N, Al-Sarraj S, Bodi I, et al. Assessment of beta-amyloid deposits in human brain: A study of the BrainNet Europe Consortium. Acta Neuropathol 2009;117:309–20.

[19] Crary JF, Trojanowski JQ, Schneider JA, Abisambra JF, Abner EL, Alafuzoff I, et al. Primary age-related tauopathy (PART): A common pathology associated with human aging. Acta Neuropathol 2014;128:755–66.

[20] Thal DR, Griffin WS, Braak H. Parenchymal and vascular Abeta-deposition and its effects on the degeneration of neurons and cognition in Alzheimer's disease. J Cell Mol Med 2008;12:1848–62.

[21] Lim YY, Maruff P, Pietrzak RH, Ames D, Ellis KA, Harrington K, et al. Effect of amyloid on memory and non-memory decline from preclinical to clinical Alzheimer's disease. Brain 2014;137:221–31.

[22] Fleisher AS, Chen K, Quiroz YT, Jakimovich LJ, Gomez MG, Langois CM, et al. Florbetapir PET analysis of amyloid-beta deposition in the presenilin 1 E280A autosomal dominant Alzheimer's disease kindred: A cross-sectional study. Lancet Neurol 2012;11:1057–65.

[23] Chetelat G, La Joie R, Villain N, Perrotin A, de La Sayette V, Eustache F, et al. Amyloid imaging in cognitively normal individuals, at-risk populations and preclinical Alzheimer's disease. Neuroimage Clin 2013;2:356–65.

[24] Villemagne VL, Pike KE, Darby D, Maruff P, Savage G, Ng S, et al. Abeta deposits in older non-demented individuals with cognitive decline are indicative of preclinical Alzheimer's disease. Neuropsychologia 2008;46:1688–97.

[25] Mattsson N, Insel PS, Donohue M, Landau S, Jagust WJ, Shaw LM, et al. Independent information from cerebrospinal fluid amyloid-beta and florbetapir imaging in Alzheimer's disease. Brain 2015;138:772–83.

[26] Thal DR, Horn M, Schlote W. Selective quantitative analysis of the intensity of immunohistochemical reactions. Acta Histochem 1995;97:203–11.

[27] Alafuzoff I, Pikkarainen M, Al-Sarraj S, Arzberger T, Bell J, Bodi I, et al. Interlaboratory comparison of assessments of Alzheimer disease-related lesions: A study of the BrainNet Europe Consortium. J Neuropathol Exp Neurol 2006;65:740–57.

[28] Landau SM, Thomas BA, Thurfjell L, Schmidt M, Margolin R, Mintun M, et al. Amyloid PET imaging in Alzheimer's disease: A comparison of three radiotracers. Eur J Nucl Med Mol Imaging 2014;41:1398–407.

[29] Alafuzoff I, Pikkarainen M, Arzberger T, Thal DR, Al-Sarraj S, Bell J, et al. Inter-laboratory comparison of neuropathological assessments of beta-amyloid protein: A study of the BrainNet Europe Consortium. Acta Neuropathol 2008;115:533–46.

[30] Snellman A, Rokka J, Lopez-Picon FR, Eskola O, Wilson I, Farrar G, et al. Pharmacokinetics of [18F]flutemetamol in wild-type rodents and its binding to beta amyloid deposits in a mouse model of Alzheimer's disease. Eur J Nucl Med Mol Imaging 2012;39:1784–95.

[31] Wong DF, Moghekar AR, Rigamonti D, Brasic JR, Rousset O, Willis W, et al. An in vivo evaluation of cerebral cortical amyloid with [18F]flutemetamol using positron emission tomography compared with parietal biopsy samples in living normal pressure hydrocephalus patients. Mol Imaging Biol 2013;15:230–7.

[32] Wolk DA, Grachev ID, Buckley C, Kazi H, Grady MS, Trojanowski JQ, et al. Association between in vivo fluorine 18-labeled flutemetamol amyloid positron emission tomography imaging and in vivo cerebral cortical histopathology. Arch Neurol 2011;68:1398–403.

[33] Rosen RF, Walker LC, Levine H 3rd. PIB binding in aged primate brain: Enrichment of high-affinity sites in humans with Alzheimer's disease. Neurobiol Aging 2011;32:223–34.

[34] Jack CR Jr, Barrio JR, Kepe V. Cerebral amyloid PET imaging in Alzheimer's disease. Acta Neuropathol 2013;126:643–57.

[35] Braak H, Braak E. Neuropathological stageing of Alzheimer-related changes. Acta Neuropathol 1991;82:239–59.

[36] Mirra SS, Heyman A, McKeel D, Sumi SM, Crain BJ, Brownlee LM, et al. The Consortium to Establish a Registry for Alzheimer's Disease (CERAD). Part II. Standardization of the neuropathologic assessment of Alzheimer's disease. Neurology 1991;41:479–86.

[37] Mackenzie IR, Neumann M, Bigio EH, Cairns NJ, Alafuzoff I, Kril J, et al. Nomenclature and nosology for neuropathologic subtypes of frontotemporal lobar degeneration: An update. Acta Neuropathol 2010;119:1–4.

[38] Yamada M. Senile dementia of the neurofibrillary tangle type (tangle-only dementia): Neuropathological criteria and clinical guidelines for diagnosis. Neuropathology 2003;23:311–7.